The Evolving Scholar Vol. 3, 2023

https://dx.doi.org/10.59490/64f21eec0b23ace23fac5785

Bicycle and Motorcycle Dynamics 2023
Symposium on the Dynamics and Control of Single Track Vehicles
18 – 20 October 2023, Delft University of Technology, The Netherlands

Type of the Paper: Conference Paper

Improvement of Cycling Efficiency for Drivetrains with Elasticity

Willem den Boer

Huron Cycling LLC, Brighton, Michigan, USA; willem@huroncycling.com, ORCID 0000-0001-9290-8320

Name of Editor: Jason Moore
Submitted: 01/09/2023
Accepted: 07/09/2023
Published: 07/09/2023
Citation: Den Boer, W. (2023). Improvement of Cycling Efficiency for Drivetrains with Elasticity. The Evolving Scholar - BMD 2023, 5th Edition.

Abstract:

Test and modeling results are reported on a bicycle crankset with limited elasticity. Like record-breaking running shoes, the crank set has spring action which mitigates the effect of the dead zone during the pedal stroke. Fiber composite leaf springs are inserted inside the hollow carbon crank arms. The crank arms are not directly attached to the crank axle. Instead, sleeve bearings allow the crank arms to rotate by up to about five degrees relative to the crank axle. The rotation is counteracted by the springs and is proportional to applied torque at the pedals. The novel crank set and a conventional crank set with forged aluminum crank arms were both tested on a stationary bike. The ratio of effective speed to input power is used as a measure of cycling efficiency. Depending on the difference in torque during the downstroke and in the dead zone, this ratio is typically a few percent higher for the novel crankset than for a conventional crankset. Multiple tests show efficiency improvements in the range of 1 to 4% at power levels of 200 W and cadence of 71 rpm with average of around 2%. Details of a test with 2.3 % improvement are presented. This would translate, for example, into a one minute advantage in a 45 minute time trial.

In an attempt to understand the test results computer modeling of bicycle speed and crank arm angular velocity vs. time was performed for non-elastic and and elastic crank arms. It is difficult to explain the test results with computer modeling unless it is assumed that conventional crank sets introduce energy losses in the drivetrain from twisting of the crank arms and flexing of the bicycle frame under load at the pedals and that these energy losses are reduced for the crank set with built-in elasticity.

Keywords: Cycling Efficiency, Bicycle Drivetrain, Bicycle Crankset

ISSN: 2667-2812

 http://dx.doi.org/10.59490/64f21eec0b23ace23fac5785

Introduction

It is well known that carbon fiber plates in running shoes provide a propulsive sensation which helps improve speed. Several brands of shoes have been using this technology to add a degree of elasticity in their state-of-the-art products. This has led to multiple world records in road and track running in recent years.

In the drivetrain of bicycles a limited degree of elasticity can be built in as well with beneficial effects, for example in the spider of the crank set (Hamamoto, 2019) or in the crank arms (den Boer, 2019-1 and Bastianelli *et al*, 2019). In figure 1 the method we adopted is shown. Fiber composite leaf springs are inserted inside the hollow carbon crank arms. The crank arms are not directly attached to the crank axle. Instead, sleeve bearings allow the crank arms to rotate by up to about five degrees relative to the crank axle. The rotation is counteracted by the leaf springs and is proportional to applied torque at the pedals. Since torque varies from a maximum during the downstroke to a minimum in the dead zone of the pedal stroke, the leaf springs inside the hollow crank arms bend and store energy during the downstroke and release this energy in the dead zone in the direction of rotation to contribute to effective torque.

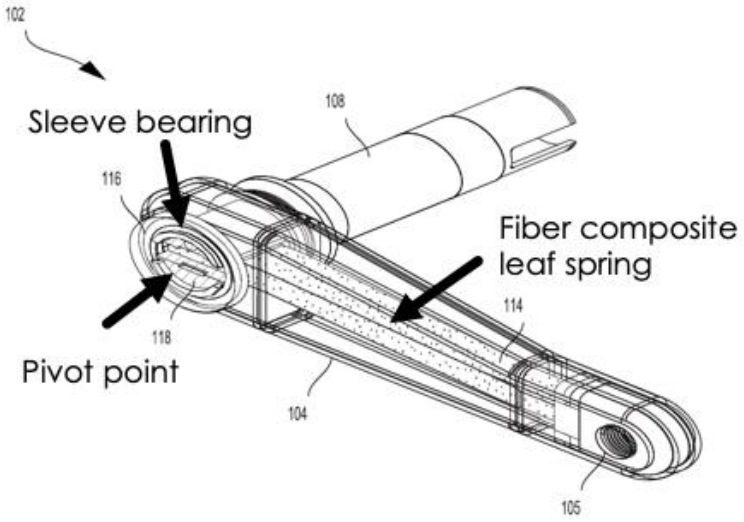

Figure 1. Cutaway view of crank arm and crank axle.

The angle of rotation θ of the crank arms relative to the crank axle is given by:

$$\theta = \frac{\tau}{k} = \frac{P}{\omega k} \tag{1}$$

where τ is the torque from the tangential force F_p applied at the pedals ($\tau = F_p * r$ with r the crank length). P is the applied power and ω is the angular velocity of the crank arms. k is a constant representing the degree of elasticity by bending of the leaf spring. For conventional cranksets without intentional elasticity the k value of the crank arms is high (Fairwheel Bikes, 2021), typically > 5000 Nm, so that θ is small. In our novel crankset k = 1000 Nm, resulting in θ = 0.07 rad (4 degrees) and a deflection at the pedals $D = \theta * r$ = 12.25 mm (0.48 inch) for a tangential force of 400 N (90 pounds). Leaf springs with different k values can be used depending on the power and skill of the cyclist.

Figure 2 shows a photograph of several crank sets based on the principle of internal leaf springs. In earlier prototypes we also used metal compression springs outside the crank arms (Bastianelli *et al*, 2019, www.huroncycling.com) for proof of concept. They are, however, too heavy for practical use.

ISSN: 2667-2812

 http://dx.doi.org/10.59490/64f21eec0b23ace23fac5785

Figure 2. Photograph of crank sets based on the design of figure 1.

Although the principle of operation of limited elasticity in bicycle drivetrains is quite different from that in running shoes, testing shows a benefit in cycling as well.

Testing

The novel crankset was installed on a carbon frame bicycle and compared with a conventional crank set with forged aluminum crank arms, while keeping the gear ratio constant at 36/17 and the slope constant at 3 %. To eliminate wind drag factors and changing conditions the testing was performed indoors on a Tacx Neo smart trainer with two power meters (see figure 3):

1. A Powertap P1 pedal power meter at left and right pedals to measure input power

2. The internal power meter of the Tacx Neo to measure effective speed

Figure 3.Test setup

Data from the smart trainer was displayed and stored on the Tacx app on a smart phone via Bluetooth wireless protocol.
The input power was measured at the pedals, both left and right, with a Powertap P1 pedal-based power meter. This power is representative of the input power applied by the left and right legs to the pedals. The information was displayed and stored on a Garmin Edge 810 head unit via ANT+ wireless protocol.

ISSN: 2667-2812

 http://dx.doi.org/10.59490/64f21eec0b23ace23fac5785

More than twenty sets of tests were performed of 15 or 30 minutes duration each with seven different prototypes of our novel crank set. To verify repeatability of the measurements each set of experiments consisted of at least two tests with the novel crankset with limited elasticity and at least two tests with the conventional crank set made of forged aluminum. All other conditions in a set of tests, such as speed target, slope setting, gear ratio) were kept identical. This allows a direct comparison of the two crank sets. Each test was performed at constant input power of around 200 W.

The speed-power ratio *SPR* was used as a measure for cycling efficiency. Percentage of change *Δ(%)* between the prototype novel crank set and the conventional crank set was defined as:

$$\Delta(\%) = \frac{SPR_{proto} - SPR_{conv}}{SPR_{conv}} \quad (2)$$

where SPR_{proto} and SPR_{conv} are the speed-power ratio for drivetrains with the prototype and conventional crank set, respectively.
Table 1 shows the input conditions for a representative test of 15 minutes. The effective speed measured on the Tacx smart trainer is based on the number of rotations of the back wheel.

Table 1. Experimental setup and conditions of typical test

Test equipment	Tacx Neo smart bike trainer
Slope setting	3 %
Power target	200 W
Duration of tests	15 minutes
Gear ratio	36/17
Power meters	Tacx Neo (better than 0.5 % accuracy)
	Powertap P1 left and right pedal power meter
Control conventional crank set	FSA Gossamer BB30 175 mm crank length
Prototype novel crank set	Leaf springs with k=1000 Nm 175 mm crank length

The conventional crank set was an FSA Gossamer BB30 unit with forged aluminum crank arms. After the control testing, the conventional crank set was replaced with the novel crank set with embedded leaf springs. The slope on the Tacx Neo was set at 3 % to prevent any freewheeling during the tests. In each test the power was ramped up to 200 W before starting the measurement and was then maintained around 200 W for the remaining time of the test.
Test results for a typical 15 minute test are shown in Table 2. Repeatability of results was within 0.5 % for each crankset and the table shows the average of two identical tests for each crank set.

Table 2. Test results around 200 Watts on Tacx Neo at 3 % slope for 15 minutes

	Conventional crank set	Novel crank set
Average Speed Tacx (km/h)	19.4	19.4
Average Cadence Tacx (rpm)	71	71
Distance Tacx (km)	4.865	4.865
Average Power Powertap P1 (Watts)	200.5	196
Energy Powertap P1 (kJoule)	180.5	176.5

As seen in Table 2, for the novel crank set the speed-power ratio is higher than for the conventional crank set. The difference *Δ(%)*, as defined in equation (2) is 2.3 %. In other words: With the novel crankset the cyclist can go faster using the same power or maintain the same speed while exerting less power. This is confirmed by the energy in kJoule comparison, which gives the same percentage difference. It takes less energy to complete the same distance at the same speed for the novel drivetrain.
The twenty sets of experimental data for seven different prototypes with k = 1000 Nm show a range of improvement *Δ(%)* of 1 to 4% as compared to the conventional crankset with forged aluminum crank arms.
The lower power needed to maintain the same speed with the novel crank set may be explained by the reduced force on the pedals during the down stroke at 3 o'clock and 9 o'clock crank angles and the release of stored energy from the springs in the dead zone.

ISSN: 2667-2812

 http://dx.doi.org/10.59490/64f21eec0b23ace23fac5785

A few tests were also performed at constant 200 W power for different cadence levels by changing the gear ratio to 36/19 and 36/15. In the range of 64 to 80 rpm the improvement with the novel drivetrain remains in the same range.
For constant cadence of about 72 rpm but lower power levels of 179 Watts (gear ratio 36/19) we still see similar improvement. When the power is further lowered to 162 Watts (gear ratio 36/21) at 72 rpm on the Tacx trainer, the improvement is reduced. This is to be expected as a result of the reduced force on the pedals and reduced torque on the crank and therefore reduced deflection at the pedals. The test results do not depend on the type of pedal-based power meter: For earlier testing a Garmin Vector power meter for left and right pedals was used with similar results as the Powertap P1.

Modeling

In an attempt to understand the effect of drivetrain elasticity on bicycle speed vs. input power, computer modeling was performed. Figure 4 shows the forces at work and the resulting speed of the bicycle. Torque τ on the pedals $\tau = F_p * r$, where r is the crank length and F_p is the tangential force on the pedal. This results in a force F_{bike} propelling the bicycle. $F_{counter}$ is the counterforce, such as wind drag or gravity going uphill. Torque varies by $\Delta\tau$ between a maximum during the downstroke and a minimum during the dead zone of the pedal stroke. $\Delta\tau$ depends on the rider style, but is typically high, even for skilled cyclists. The novel crank set makes a difference only if $\Delta\tau$ is nonzero, i.e. when the springs are alternatingly storing and releasing energy.

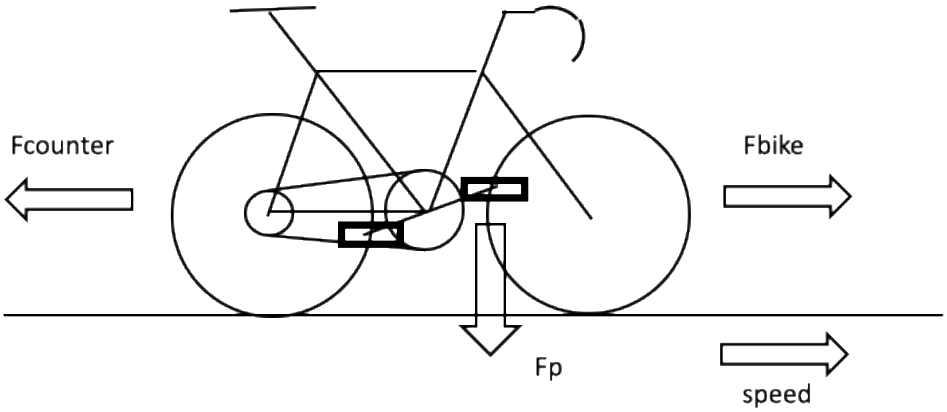

Figure 4. Forces at work on a bicycle

Measurements of torque vs crank angle by us (den Boer, 2019-2) and many power meter manufacturers show that the combined power P applied at left and right pedals is approximately sinusoidal with a frequency twice the crank rotation frequency. In the following P is assumed to vary between a maximum during the downstroke and zero at the dead spot:

$$P = P_0 (\sin \beta)^2 = P_0(1 - \cos(2\beta))/2 \tag{3}$$

where β is the crank angle and P_0 is the maximum power during the downstroke when β = 90 degrees. At $t = 0$ the crank angle is in the vertical position of one of the cranks. The torque τ on the crank axle is:

$$\tau = \frac{P}{\omega} \tag{4}$$

where ω is the angular velocity of the crank arms. The force propelling the bicycle is given by:

$$F_{bike} = \frac{P}{v} \tag{5}$$

The change in speed dv of the bicycle from a starting velocity of v_0 is given by Newton's law:

$$\mathrm{d}v = \frac{F_{net} * \mathrm{d}t}{m} \tag{6}$$

ISSN: 2667-2812

 http://dx.doi.org/10.59490/64f21eec0b23ace23fac5785

where F_{net} is the net force on the bicycle ($F_{net} = F_{bike} - F_{counter}$), dt is the time step in the calculation and m is the combined mass of rider plus bike. In an iterative numerical calculation F_{bike} and v can be calculated vs time. The time step dt can be reduced to ensure it is small enough to not impact the calculated results.

In the following the counterforce is gravity on an uphill slope with angle α:

$$F_{counter} = mgsin\alpha \tag{7}$$

where g is the gravitational acceleration (g = 9.81 m/s^2)

Modeling of conventional drivetrain without elasticity

For a drivetrain without any elasticity the angular velocity of the crank arms and velocity of the bicycle are directly related to each other:

$$v = \omega * R * GR \tag{8}$$

where R is the rear wheel diameter and GR is the gear ratio between front chainring and back cog. The following is an example calculation for the following input parameters:

m = 70 [kg]
v_0 = 1 [m/s]
P_0 = 500 [W] for an average power of 250 W
R = 0.35 [m]
GR = 2
r = 0.175 m
Uphill slope α = 0.1 rad, corresponding to 5.72 degrees or 10 %

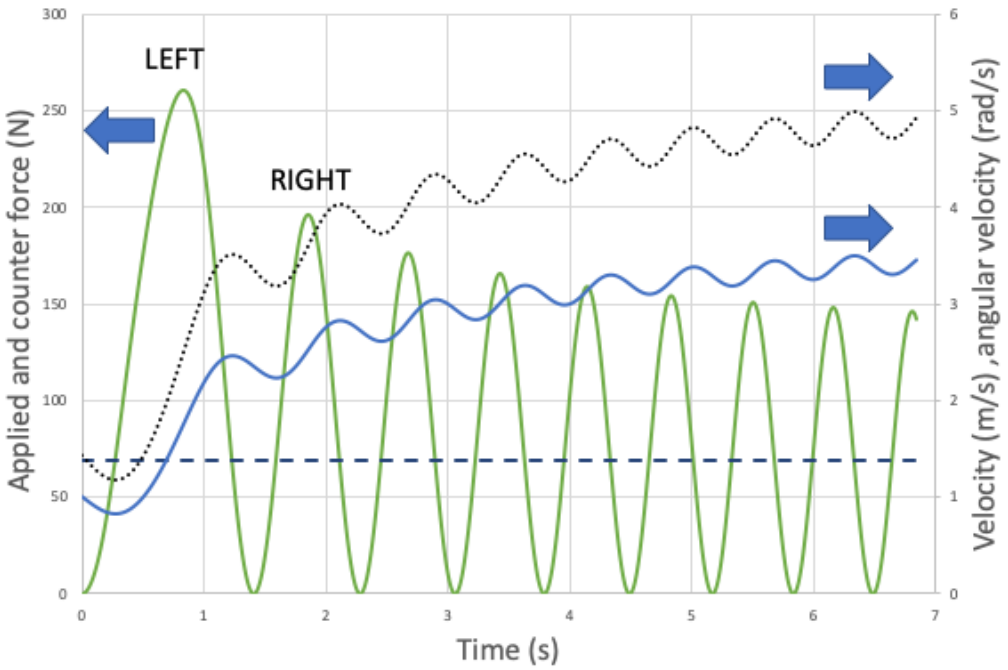

Figure 5. Example of calculated F_{bike}, $F_{counter}$ (dashed line) and velocity and angular velocity (dotted line) vs. time for a drivetrain without elasticity. LEFT and RIGHT represent alternatingly left and right pedal.

ISSN: 2667-2812

 http://dx.doi.org/10.59490/64f21eec0b23ace23fac5785

In figure 5 the results are shown for the applied force F_{bike} to the bike and the resulting velocity of the bike and angular velocity of the cranks vs. time. $F_{counter}$ is constant at 68.5 N. Both F_{bike} and v oscillate. The velocity increases from 1 m/s to an average of about 3.65 m/s when the pace stabilizes. In the final steady state the average F_{bike} and $F_{counter}$ cancel each other out. After the pace settles to its final value, v still oscillates as a result of the varying torque on the crank axle. There is a phase delay of about 45 degrees between the maxima in angular velocity and applied force, because velocity continues to increase as long as net force is positive. This phase delay is well-documented in measurements of angular velocity profiles by power meters (see e.g. www.favero.com) and is the result of the varying torque applied by the rider at the pedals. For a perfectly rigid drivetrain without any elasticity the oscillations in bicycle velocity v are, percentagewise, the same as the oscillation in angular velocity of the crank arm, in agreement with equation (8). The amplitude of the velocity oscillations is proportional to the torque variation $\Delta\tau$ during the pedal stroke and inversely proportional to cadence (i.e. to average angular velocity at constant pace). The dependence on cadence is shown in figure 6 where the velocity oscillations in percent are defined as:

$$\Delta v\ (\%) = \frac{v_{max} - v_{min}}{v_{max} + v_{min}} \tag{9}$$

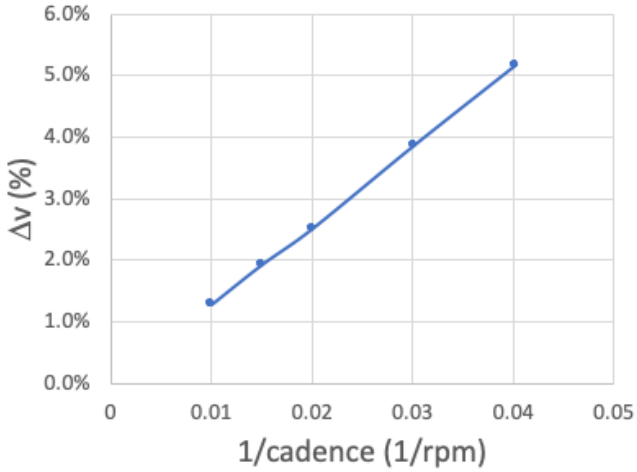

Figure 6. Dependence of velocity oscillations on cadence

It is well-known that the most energy-efficient way to travel is at constant velocity. If the velocity oscillates, the power required to maintain the average final speed of 3.65 m/s (the pace) increases, as a result of the quadratic dependence of kinetic energy on velocity. One of the purposes of the modeling was to find out if these velocity oscillations are reduced when there is elasticity in the drivetrain, since, if this is the case, this could explain the test results at least partially.

Modeling of drivetrain with elasticity

When the bicycle drivetrain has limited spring action, i.e. some degree of elasticity, equation (8) is no longer valid. Even when the gear ratio GR is fixed, the angular velocity of the cranks is not exactly proportional to the speed of the bicycle. In the case of the crank set of figure 1 limited elasticity is achieved by leaf springs inside the hollow crank arms. The angles of the left and right crank arms are no longer the same as the angle of the crank axle. During the downstroke energy is stored in the spring, which is then released in the dead spot in the direction of rotation. This contributes to torque on the crank axle close to the dead spot. The instantaneous applied power to the pedals is no longer equal to the power to propel the bike as a result of the temporary energy storage in the springs. Figure 7 shows the effect of the springs on the crank and crank arm angles

ISSN: 2667-2812

 http://dx.doi.org/10.59490/64f21eec0b23ace23fac5785

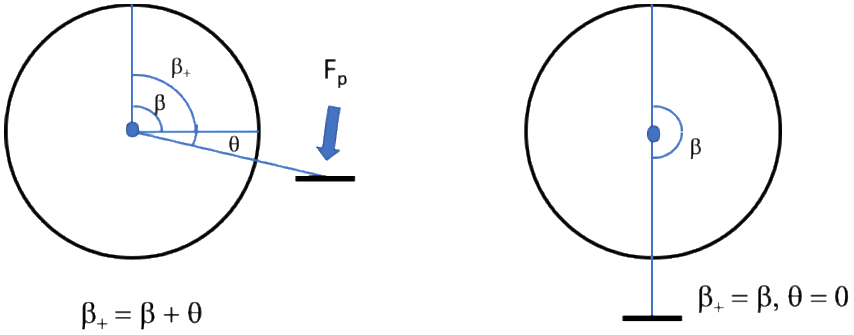

Figure 7. Deflection θ of the crank arm with elasticity, at left during the downstroke, at right in the dead spot

At applied torque τ at the pedals the crank arm deflects by an angle θ:

$$\tau = F_p * r = k\theta \tag{10}$$

where k is the spring constant of the fiber composite leaf spring inside the hollow crank arm and θ is the deflection angle of the crank arm at torque τ. As a result the angle β_+ of the crank arms is different from the angle of the crank axle β and is augmented with the deflection angle θ:

$$\beta_+ = \beta + \theta \tag{11}$$

In the dead spot the leaf spring releases its stored energy and the angle θ decreases to zero if the torque decreases to zero. The angular velocity ω_+ of the crank arm also becomes different from the angular velocity ω of the crank axle:

$$\omega_+ = \frac{d\beta_+}{dt} = \omega + \frac{d\theta}{dt} \tag{12}$$

The tangential pedal force F_p is now:

$$F_p = \frac{P}{\omega_+ r} \tag{13}$$

The energy E_{spring} stored in the spring is given by:

$$E_{spring} = \frac{1}{2} k\theta^2 \tag{14}$$

The power P_{spring} is added to P and is the negative derivative of E_{spring}. It is negative when the spring is loaded, i.e. when θ increases, and positive when the spring relaxes, i.e. when θ decreases:

$$P_{spring} = -\frac{dE_{spring}}{dt} = -k\theta \frac{d\theta}{dt} \tag{15}$$

The force F_{spring} exerted by the spring at the pedals is added to the force applied bythe cyclist:

$$F_{spring} = \frac{P_{spring}}{\omega_+ r} \tag{16}$$

ISSN: 2667-2812

 http://dx.doi.org/10.59490/64f21eec0b23ace23fac5785

Using equations (3), (10), (15) and (16) it can be shown that:

$$F_{spring} = -F_p * \frac{P_0 \sin(2\beta)}{\omega_+ k} \tag{17}$$

The force F_{ax} applied to the crank axle is:

$$F_{ax} = F_p + F_{spring} = F_p(1 - \frac{P_0 \sin(2\beta)}{\omega_+ k}) \tag{18}$$

When only the crank arms have elasticity and the rest of the drivetrain is inelastic, the forward force applied to the bicycle, becomes:

$$F_{bike} = \frac{F_{ax} * r}{R * GR} \tag{19}$$

Very high values of k represent conventional crank sets with little elasticity, when F_{ax} is almost equal to F_p in equation (18). The difference between F_{ax} and F_p is small, even for elastic crank arms with k = 1000 Nm. However, the difference in the angular velocity fluctuations of the cranks is significant. For the conditions of the simulation listed earlier the angular velocity of, alternatingly, the left and right crank arms and the crank axle are actually out of phase with each other, as shown in figure 8. The speed of the bicycle and the crank axle angular velocity still track each other because there is no elasticity in the drivetrain between the crank axle and the rear wheel. F_p and F_{bike} no longer track each other exactly as a result of energy storage in the springs.

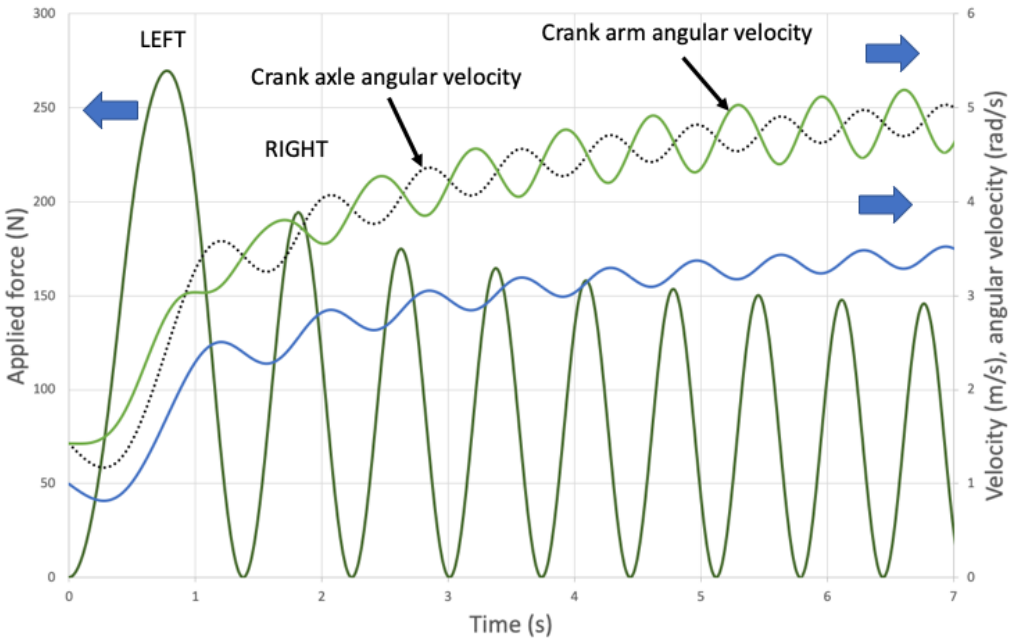

Figure 8. Calculated F_{bike}, velocity and angular velocities vs. time for the drivetrain with elasticity

Calculation of speed-power ratio

The ratio of average speed to input power was calculated at constant pace for inelastic and elastic drivetrains. Although the angular velocity profile of the crank arms changes significantly when elasticity is introduced, as shown in figure 8 , we do not see much change in the speed-power ratio at constant pace, certainly not enough to explain the experimental results. Bicycle velocity oscillations do not change much, when elasticity is introduced into the drivetrain. Therefore they cannot explain the observed test

ISSN: 2667-2812

results, unless there are significant delays in the energy release of the leaf springs. This was not considered yet, because the resonance frequency of the springs is much larger than the pedaling frequency. In the case of loss-free crank sets, only a large reduction of oscillations in the bicycle velocity would reduce power input. This large reduction is not seen in the modeling to date. More accurate modeling, considering the delay in reaction to forces on the springs, may give only slightly different results.

Losses in conventional crank sets

The modeling above shows that speed/power ratio does not significantly change when elasticity is introduced in the drivetrain. This is attributed here to the assumption that there are no losses in a conventional crankset. It is, however, well known that during large force on the pedals during the downstroke the bicycle frame can be flexed significantly in a lateral direction (ACT Lab, 2017). In the dead spot the frame flexes back but the energy used in flexing is not returned to effective torque on the crank axle and therefore lost for propulsion. Similarly, the load on the pedal several centimeters away from the crank arm causes twisting of the crank arms (ACT Lab, 2016) during the downstrokes. Again, the energy used for twisting is not recovered in the dead spot and therefore lost.

The strain energy losses from twisting in conventional crank arms can amount to more than 1.6 % at a cadence of 100 rpm (Fairwheel Bikes, 2021) and even more at lower cadence for the same power input. We argue that in our crank set with leaf springs the strain energy on the crank arms is mostly absorbed in the leaf springs before flexing the frame and twisting the crank arms. It is then returned without significant losses in the dead spot. Since the applied force and torque in figures 5 and 8 are not very different, twisting of the crank arms is a more likely cause.

Modeling of drivetrains with loss

To simplify modeling the flexing of the frame and twisting of the crank arms during the downstroke are combined in the degree of deformation D :

$$D = \frac{\tau}{q} \tag{20}$$

where τ is again the torque applied to the crank arms and q is the combined constant for flexing the frame and twisting the crank arms. The energy E_{def} stored during this deformation is, analogous to equation (14), given by:

$$E_{def} = \frac{1}{2} q D^2 \tag{21}$$

The total power applied to propel the bike, P_{bike} , is then:

$$P_{bike} = P + P_{spring} + P_{def} \tag{22}$$

When the strain on the frame and crank arms is reduced approaching the dead spot, P_{def} is zero, because this strain energy is not returned into effective torque on the crank axle:

$$P_{def} = -qD\frac{dD}{dt} \quad \text{if } dD/dt > 0 \tag{23}$$

$$P_{def} = 0 \quad \text{if } dD/dt < 0 \tag{24}$$

This means that P_{def} is always negative or zero and therefore reduces the power applied to propel the bike. We argue that the presence of the springs in the crank arms significantly reduces the flexing of the frame and the twisting of the crank arms, as compared to a conventional crank set. In other words, the deformation of the springs, which is reversible and contributes to propulsion in the dead spot, replaces, at least partially, the deformation of frame and crank arms. Irreversible losses are replaced by reversible losses.

For the conventional crankset $P_{spring} = 0$, so it does not have the elasticity to absorb the same losses. For example, if he deformation energy $\frac{1}{2} qD^2$, when using a conventional crankset is the same as the energy stored in the leaf springs $\frac{1}{2}k\theta^2$, the model shows that for the parameters listed above the pace at 250 W average input power is reduced from 3.65 to 3.5 m/s, for a 2.8 % reduction in speed/power ratio. In the novel crankset the deformation energy would be, at least partially, replaced by reversible energy loss in the leaf springs, keeping the pace closer to 3.65 m/s and the speed/power ratio higher.

ISSN: 2667-2812

Conclusions

Test results have been presented indicating that a bicycle drivetrain with elasticity in the crank arms can improve cycling efficiency, as reported by others as well (Bastianelli *et al*., 2019). For the conditions used in one particular test, an increase of 2.3 % in the speed-power ratio of our bicycle with a crank set including leaf springs was measured. In a 45 minute time trial this would translate into more than one minute advantage, a large improvement compared with the more incremental benefits from aerodynamic optimization.

Our computer modeling to date cannot explain the test results unless energy losses are assumed in conventional crank sets from flexing the bicycle frame and twisting the crank arms during the downstroke. We argue that in a drivetrain with limited elasticity these irreversible losses during the downstroke are reduced and partially converted into reversible losses in the leaf springs. More testing is recommended on elastic drivetrains in general to verify and confirm our test results, as well as measurements of cranksets with elasticity in the spider (Hamamoto, 2019). Elasticity in the drivetrain can also be introduced by using stretchable drive belts instead of chains.

Other explanations than presented here are possible based on more advanced computer modeling. FEA modeling with all the material constants involved may be needed to obtain more quantitative results.

References

ACT Lab (2016), Crank Fatigue Test, https://www.youtube.com/watch?v=7rZ1L6brkNE

ACT Lab (2017), Frame Fatigue with Pedalling Forces Test, https://www.youtube.com/watch?v=8blo6O_KIAs

Bastianelli, B. M., Workman, A. & McGregor, S. (2019, June), Novel Crank with Elastomer Spring Improves Effective Power in Trained Cyclists and Triathletes, *Medicine & Science in Sports & Exercise*, Chicago, 2019, 51(6S):p 942-943, June 2019.

den Boer, W. (2019-1), US Patent 11,142,281, Cycle Crank Assembly, www.huroncycling.com

den Boer, W. (2019-2), White Paper IMPACT power meter August 2019: www.huroncycling.com

Fairwheel Bikes (2021), https://blog.fairwheelbikes.com/reviews-and-testing/road-bike-crank-testing/

Hamamoto, Y. (2019), US Patent 10,450,030, Rotational Apparatus and Bicycle provided with same, www.olympic-corp.co.jp/cycle/freepower/en

ISSN: 2667-2812